Journal of Thermal Analysis, Vol. 47 (1996) 1709-1718

THERMAL STABILITY AND NON-ISOTHERMAL DECOMPOSITION KINETICS OF A POLYNUCLEAR COORDINATION COMPOUND PRECURSOR OF COPPER FERRITE

Oana Carp[*], *Maria Brezeanu*[**] *and E. Segal*[***]

[*]Institute of Physical Chemistry, Splaiul Independentei nr. 202, Sector 6, Bucharest
[**]Department of Inorganic Chemistry, Faculty of Chemistry, University of Bucharest, Dumbrava Rosie Str., Nr. 23, Bucharest
[***]Department of Physical Chemistry, Faculty of Chemistry, University of Bucharest, Bd. Carol I, nr. 12, Bucharest, Romania

(Received January 2, 1995; in revised form December 20, 1995)

Abstract

Results are presented on the thermal behaviour of $[Fe(III)_2Cu(C_2O_4)_2(OH)_4(H_2O)_2]$ precursor of copper ferrite. An investigation of the decomposition steps and intermediates was followed by a non-isothermal kinetic analysis of the processable steps.

Keywords: kinetics

Introduction

The most common method for the preparation of mixed oxides is the ceramic one. One of the new chemical methods used to obtain these oxides with a specific composition is the thermal decomposition of solid polynuclear coordi- nation compounds [1]. This method has the advantage of yielding reproducible products with high purity and homogeneity.

We earlier [2–4] reported results on the thermal decomposition of some polynuclear coordination compounds obtained through forced hydrolysis, used as precursors of ferrite spinels.

In order to obtain more information on this 'non-traditional' method, we have now extended our investigations to other spinel ferrites with other 3*d* metals. The present paper deals with the thermal decomposition of a polynuclear coordination compound containing iron and copper in a stoichiometric ratio of 2:1.

0368–4466/96/ $ 5.00

John Wiley & Sons, Limited
Chichester

Experimental

The polynuclear coordination compound, a precursor of an iron-copper mixed oxide, was obtained by hydrolytic decomposition of the system $Fe_2C_2O_4{\cdot}2H_2O$–$Cu(CH_3COOO)_2{\cdot}2H_2O$, with a Fe:Cu molar ratio of 2:1 [5]. The compound obtained corresponds to the composition described by the formula $[Fe(III)_2Cu(C_2O_4)_2(OH)_4(H_2O)_2]$.

The separated compound was characterized by chemical analysis, magnetic susceptibility measurements, IR and electronic spectra and X-ray powder diffraction data [5].

The crystalline state of the polynuclear coordination compound was investigated by using a DRON 3 X-ray diffractometer with CoK_α radiation.

The thermal decomposition curves were recorded with a Q-1500 D Paulik-Paulik-Erdey derivatograph in a static air atmosphere, with α-Al_2O_3 as inert reference compound, at heating rates in the range 0.6–10 K min^{-1}. The sample mass used in the non-isothermal kinetic study was 0.100±0.01 g.

For each reaction step, we determined the temperature range of occurrence, the kinetically processable conversion intervals, the most probable decomposition mechanism, the non-isothermal kinetic parameters (pre-exponential factor A and activation energy E) and the rate constant k (corresponding to a temperature in the temperature range of reaction occurrence). These results were obtained by processing the thermogravimetric data with the programs DISCRIM 1 [6] and DISCRIM 2 [7].

The purity of the final decomposition product was checked by chemical analysis, and ferrite phase formation was evidenced by using X-ray diffraction and magnetic susceptibility measurements [8].

Results and discussion

A. Reaction stoichiometry

The formulation of the polynuclear coordination compound as $[Fe(III)_2Cu(C_2O_4)_2(OH)_4(H_2O)_2]$ was confirmed by chemical and physicochemical analyses.

Its electronic spectrum contains absorption maxima which may be assigned to the *d-d* transitions of $[Fe(III)O_6]^{-3}$ and $[Cu(II)O_4]^{-2}$ [9].

The IR spectrum shows that the positions of band maxima assigned to the vibrational modes of the oxalate in the polynuclear coordination compound are very close to those obtained for $FeC_2O_4{\cdot}2H_2O$. This indicates the same function of the oxalate anions (double bridged between two metallic ions) and the not strongly modified character of the C–O linkages (in spite of the interactions with the metal ions).

Table 1 X-ray powder diffraction data

Number of line	(hkl)	$FeC_2O_4{\cdot}2H_2O$ ASTM 23-293		$[Fe(III)_2Cu(C_2O_4)(OH)_4(H_2O)_2]$	
		$d/Å$	I/I_o	$d/Å$	I/I_o
1	111 002	4.80	100	4.851	100
2	200	4.70	65	4.731	79
3	$\bar{2}02$	3.880	25	3.881	59
4	$\bar{1}12$	3.629	20	3.629	8
5	$\bar{2}11$	3.597	25	3.595	17
6	211	3.172	4	3.067	7
7	202	3.004	50	2.995	53
8	020	2.778	4	2.722	2
9	$\bar{2}13$	2.654	30	2.650	16
10	$\bar{3}12$	2.634	16	2.638	6
11	$\bar{1}21$	2.616	25	2.616	15
12	$\bar{2}04$	2.396	3	2.398	4
13	$\bar{4}02$	2.355	3	2.356	3
14	$\bar{2}22$	2.258	13	2.259	11
15	$\bar{4}11$	2.224	3	2.230	3
16	213	2.190	4	2.193	3
17	$\bar{1}23$	2.122	9	2.131	11
18	$\bar{3}21$	2.106	8	2.036	8
19	$\bar{3}14$	2.047	7		
20	$\bar{4}13$	2.021	14		
21	123	1.980	3	1.983	2
22	204	1.949	11	1.947	9
23	402	1.929	9	1.928	8
24	$\bar{3}23$	1.893	15	1.896	7.5
25	$\bar{2}15$	1.847	2	1.856	2
26	$\bar{5}12$ 015	1.816	21	1.817	4
27	430	1.795	4	1.793	7

The X-ray powder diffractogram of the polynuclear coordination compound $[Fe(III)_2Cu(C_2O_4)_2(OH)_4(H_2O)_2]$ reveals the formation of a strongly crystalline product. Its lattice is isomorphous with that of $FeC_2O_4{\cdot}2H_2O$ (used as starting material). Table 1 lists the Miller indices, the interplanar distances (*d*) and the relative intensities corresponding to the diffraction lines of the two mentioned substances. The crystalline size for the most intense line of the polynuclear coordination compound, calculated by using Scherrer's formula [10], is $l=310$ Å.

The fact that the monoclinic structure of the $FeC_2O_4 \cdot 2H_2O$ used as starting material is preserved in the polynuclear coordination compound could be evidence that its formation takes place through the intrusion of Cu(II) ions in the ferrous oxalate lattice.

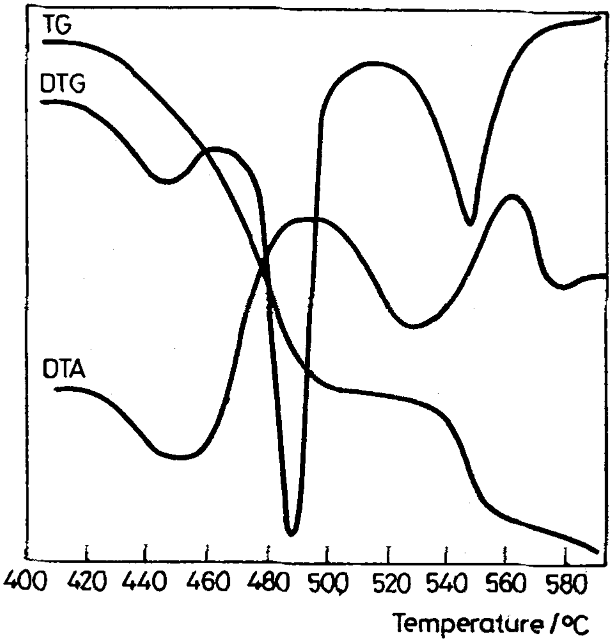

Fig. 1 Thermoanalytical curves for the polynuclear compound ($\beta=5$ K min^{-1})

The thermal curves obtained for the decomposition of the polynuclear coordination compound are given in Fig. 1.

The thermogravimetric data indicate that the polynuclear coordination compound $[Fe(III)_2Cu(C_2O_4)_2(OH)_4(H_2O)_2]$ undergoes the following reaction steps in the temperature range 293–573 K

$$[Fe(III)_2Cu(C_2O_4)_2(OH)_4(H_2O)_2]\ (s) \xrightarrow{418-471\ K} [Fe(III)_2Cu(C_2O_4)_2(OH)_4]\ (s) + 2H_2O\ (g) \qquad (I)$$

$$[Fe(III)_2Cu(C_2O_4)_2(OH)_4]\ (s) \xrightarrow{471-513\ K} Fe(III)_2Cu(CO_3)_2O_2\ (s) + 2H_2O\ (g) + 2CO\ (g) \qquad (II)$$

$$Fe(III)_2Cu(CO_3)_2O_2\ (s) \xrightarrow{533-573\ K} Fe_2CuO_4\ (s) + 2CO_2\ (g) \qquad (III)$$

The temperatures above the arrows denote the range in which each reaction occurred during heating at $\beta = 5$ K min^{-1}.

The experimental total mass loss recorded from the TG data is 45.35%, which compares well with the theoretical values of 44.99%.

The thermal transformation of the polynuclear coordination compound into the mixed oxides requires more than one stage:

a. thermal decomposition of the polynuclear coordination compound with the formation of amorphous product(s);

b. crystallization of the amorphous products with subsequent formation of the crystalline oxides;

c. solid-state reaction of the crystalline simple oxides with the formation of mixed oxides (ferrites).

Separation of these steps is rather difficult and not always possible. Since the cations are already mixed in a single precursor phase on an atomic scale (being hardly 10 Å apart), stages b and c are often superimposed, and ferrite formation from the simple crystalline oxides occurs simultaneously with their crystallization.

The final product of the decomposition, which corresponds to the molecular formula of copper ferrite (Fe_2CuO_4), is amorphous. The spinel lattice is formed by heating the decomposition product at different temperatures. Calcination at 900°C (3 h), followed by slow cooling down to room temperature, leads to the formation of a tetragonal ferrite with structural and magnetic properties close to the theoretical values (Table 2).

Table 2 Structural and magnetic characteristics obtained for tetragonal ferrite (reaction product)

	Cell's parameters		μ_{exp}
	a/Å	*b*/Å	(MB)
Decomposition's product calcined at 900° (3 h), slowly cooled	5.857	8.603	1.22
Literature data	5.844 [11]	8.630 [11]	1.23 [12]

B. Reaction kinetics

A kinetic analysis of the thermal decomposition must include a consideration of the possible changes in the reaction mechanism during its occurrence. In order to do this, we determined the non-isothermal activation parameters (pre-

Table 3 Non-isothermal kinetic parameters values for the range $0 < \alpha < 1$ and significant portions of (α, T) curve (β=5 K min^{-1})

α–range	T_i^*/K T_f^*/K	T_{max}^*/K	Computation of $f(\alpha)$ program	$f(\alpha)$	A/ s^{-1}	E/ kJ mol–1	$k\cdot 10^2$/ s–1	Mean square deviation
(I). The rate constant k is calculated at 446 K								
	418			contracting sphere	3.46×10^{9}	88.2	61.7	3.46
0–1	–	448	DISCRIM 2					
	471			contracting cylinder	9.78×10^{9}	58.9	58.9	7.15
			DISCRIM 1	$(1-\alpha)^n$ n=0.64	2.90×10^{10}	93.3	29.7	2.49
	418			contracting sphere	9.35×10^{12}	111.0	93.4	0.38
0–α_{ip}	–		DISCRIM 2					
(0–0.4546)	448			contracting cylinder	2.90×10^{12}	107.9	14.8	0.44
	448			contracting sphere	8.01×10^{8}	83.6	77.7	2.40
α_{ip}–1	–		DISCRIM 2					
(0.4546–1)	471			contracting cylinder	9.26×10^{7}	75.9	83.2	3.37
	427			contracting sphere	8.50×10^{12}	114.4	29.7	0.18
Accelerator period	–		DISCRIM 2					
(0.1142–0.4546)	448							
	418			power law	0.77×10^{15}	139.1		0.94
Induction period			DISCRIM 2					
(0–0.1142)	427			$1/n\alpha^{n-1}$ n=2	9.78×10^{9}			

Table 3 Continued

α-range	T_i^*/K T_f^*/K	T_{max}^*/K	Computation of $f(\alpha)$ program	$f(\alpha)$	A/ s^{-1}	E/ kJ mol^{-1}	$k \cdot 10^2$/ s^{-1}	Mean square deviation
(II). The rate constant k is calculated at 488 K								
0–1	471 – 513	488	DISCRIM 2	$(1-\alpha)$	1.54×10^{17}	162.3	15.9	7.32
			DISCRIM 1	$(1-\alpha)^{1.1}$	4.33×10^{16}	158.9	26.4	1.25
$0-\alpha_{ip}$ (0–0.4868)	471 – 488		DISCRIM 2	$(1-\alpha)$	1.75×10^{19}	183.2	24.0	1.72
$\alpha_{ip}-1$ (0.4868–1)	488 – 513		DISCRIM 2	$(1-\alpha)$	7.78×10^{11}	107.0	27.6	3.22
Accelerartory period (0.1547–0.4868)	478 – 488		DISCRIM 2	$(1-\alpha)$	1.16×10^{23}	208.7	56.3	2.04
Induction period (0–0.1547)	471 478		DISCRIM 2	power law $1/n\alpha^{n-1}$ $n=3/2$	1.62×10^{29}	271.3		0.50

Table 3 Continued

α-range	T_i^*/K T_f^*/K	T_{max}^*/K	Computation of $f(\alpha)$ program	$f(\alpha)$	A/ s^{-1}	E/ kJ mol^{-1}	$k\cdot10^2$/ s^{-1}	Mean square deviation
(III). The rate constant k is calculated at 552 K								
	533		DISCRIM 2	contracting sphere	1.26×10^{21}	226.9	15.9	4.33
0–1	–	552						
	573			contracting cylinder	7.26×10^{24}	269.9	47.9	5.09
			DISCRIM 1					
	533		DISCRIM 2	contracting sphere	1.26×10^{28}	315.9	66.0	0.75
$0-\alpha_{ip}$	–							
(0–0.3034)	552			contracting cylinder	7.26×10^{27}	300.7	39.9	0.84
	552			contracting sphere	4.56×10^{23}	232.4	42.0	1.56
$\alpha_{ip}-1$	–		DISCRIM 2					
(0.3034–1)	573							

T_i=initial temperature of reaction
T_f=final temperature of reaction
T_{max}=temperature of the inflexion point where the reaction rate reaches its maximum value.

exponential factor A and activation energy E) both for the whole range of conversion ($0<\alpha<1$) and for significant limited ranges: the intervals $0<\alpha<\alpha_{ip}$ and $\alpha_{ip}<\alpha<1$, where the subscript *ip* means the inflexion point in the curve considered. For the curves for which an induction period was clearly evidenced, the values of the non-isothermal kinetic parameters were evaluated for this period and the acceleratory phase stage (the period following the induction period up to $\alpha=\alpha_{ip}$).

Table 3 lists the values of the non-isothermal kinetic parameters (corresponding to the most probable mechanism) obtained for the experiments performed at a heating rate of $\beta=5$ K min^{-1}. Besides the results corresponding to the whole (α,T) curve, the Table also lists those corresponding to the significant portions of the (α,T) curve.

The results obtained concerning the non-isothermal decomposition kinetics and the relationship of the non-isothermal kinetic parameter values with the heating rates can be summarized as follows:

– The mechanisms determined for the whole range of conversion ($0<\alpha<1$) are preserved in the conversion ranges $0<\alpha<\alpha_{ip}$, $\alpha_{ip}<\alpha<1$ and also in the acceleratory period.

– Even if there are differences between the values of the non-isothermal kinetic parameters calculated over the whole conversion interval with respect to those obtained for the significant portions of the (α,T) curve, the rate constants k (calculated for a common temperature) are relatively close, obviously due to a compensation effect. This compensation effect is mentioned in the literature [13, 14] for many decomposition reactions, especially if they are followed under non-isothermal conditions.

– Reactions (I) and (III) occur in according to a contracting geometry mechanism (contracting cylinder and sphere), with comparable probabilities for the two models.

– For reaction (II), the most probable law describing its occurrence is $f(\alpha)=(1-\alpha)^n$, where the reaction order n equals unity.

– The induction period, when detected, is described by a powder law $\alpha=kt^n$, with $n=2$ or 3/2 [reactions (I) and (II)].

Conclusions

1. The thermal stability of the polynuclear coordination compound $[Fe(III)_2Cu(C_2O_4)_2(OH)_4(H_2O)_2]$ was investigated.

2. The non-isothermal kinetic parameters (pre-exponential factor A and activation energy E) of the three decomposition steps of this polynuclear coordination compound were determined.

3. The mechanism determined for the whole range of conversion is preserved in the significant portion of the (α,T) curve.

References

1 Maria Brezeanu, Luminita Patron and M. Andruh, 'Polynuclear Coordination Compounds and their Application' (in Romanian) Ed. Academiei, 1986.

2 Oana Carp and E. Segal, Luminita Patron, Ruxandra Barjega, C. Craiu and N. Stanica, Thermochim. Acta, 228 (1993) 249.

3 Oana Carp, E. Segal, Maria Brezeanu, Luminita Patron, Ruxandra Barjega and N. Stanica, Thermochim. Acta, 243 (1994) 43.

4 Oana Carp, E. Segal, Maria Brezeanu, Luminita Patron, C. Craiu and N. Stanica, Thermochim. Acta (in press).

5 Maria Brezeanu, Ariana Antoniu, Luminita Patron, Oana Carp, C. Lepadatu, M. Andruh and Florica Zalaru, Catalina Achim, Adriana Gheorghe, Ruxandra Barjega, Rev. Roum. Chim. (in press).

6 T. Coseac and E. Segal, Thermochim. Acta, 149 (1989) 189.

7 Oana Carp and E. Segal. Thermochim. Acta, 185 (1991) 111.

8 Maria Brezeanu, Ariana Antoniu, Luminita Patron, Oana Carp and M. Andruh, Rev. Roum. Chim. (in press).

9 C. Ballhausen, 'Introduction to Ligand field Theory' N. Y., Mc-Graw-Hill, 1962. Ch. 10.

10 H. Klug and L. E. Alexander, 'X-ray Diffraction Procedure' Eds. John Wiley & Sons, New York 1962, p. 461.

11 ASTM 34–425.

12 V. L. Snoek, J. Phys. et Radium, 12 (1951) 237.

13 E. Segal and D. Fatu, 'Introduction in Nonisothermal Kinetics' Publishing House of the Roumanian Academy, Bucharest, 1983.

14 K. Ninan, J. Thermal Anal., 35 (1989) 1267.